Superfluidity inside carbon nanotubes

Leonid. V. Mirantsev*

Institute for Problems of Mechanical Engineering, Russian Academy of Sciences, 199178, Bolshoi 61, V. O., St. Petersburg, Russia

(Received 27 March 2019; published 13 August 2019)

Molecular dynamics simulations of equilibrium structures and flows of nonpolar argon atoms confined by single-walled carbon nanotubes (SWCNTs) with circular cross section and rectangular cross section having the same area and the ratio between its sides 1 : 4 have been performed. It has been shown that, inside these SWCNTs, argon atoms form the spatially ordered structures and, under action of external driving forces they move collectively along SWCNT's axes. It has been also obtained that there are two regimes of such collective movement. In the first regime, when the driving external force f_{x0} is lower than a certain critical value f_{xc}, argon atoms flow through these SWCNTs with the finite average flow velocity. In the second regime, when the driving external force f_{x0} exceeds f_{xc}, the retarding friction force acting on argon atoms from bounding wall carbon atoms gradually drops to zero and the average flow velocity exhibits an unlimited growth. Moreover, when the retarding friction force becomes close to zero, the fluid will continue to flow with the same constant velocity at switched off external driving force. Hence, in the second regime, argon atoms inside the above-mentioned SWCNTs demonstrate the ballistic frictionless flows which resemble the superfluidic liquid flow. It has been shown that collective frictionless ballistic flows of argon atoms through SWCNTs are caused by the crystalline structure of SWCNT's bounding walls and, for the same SWCNTs with random distribution of carbon atoms on the bounding walls, one can observe only the first regime of the argon atom flows.

DOI: 10.1103/PhysRevE.100.023106

I. INTRODUCTION

Two remarkable phenomena, namely, the superfluidity and the superconductivity, are results of collective movement of ^{4}He atoms and Cooper electronic pairs, respectively [1]. Because of their collective movement, ^{4}He atoms must be scattered by boundary walls of a certain channel simultaneously and, since this process is extremely improbable, the ^{4}He fluid, or more precisely the condensed fraction of it, flows without any apparent friction. Similarly, the collective movement of Cooper electronic pairs prevents their scattering by impurities, dislocations, grain boundaries, and lattice vibrations (phonons). As a result, the electric current can flow through superconductors with no resistance at all. Both the ^{4}He atoms and Cooper electronic pairs have the total spins equal to zero, i.e., they are bosons, and their possible states are governed by the Bose statistics. The system of such particles would undergo at some very low temperature T_0 a phenomenon known as the Bose condensation. Below this temperature a finite fraction of bosons can occupy a single state with lowest energy, and these bosons are described by a single coherent quantum mechanical wave function, and, as a result, they can move collectively, i.e., as a whole. As the temperature is lowered, the fraction of condensed boson particles increases, and at the absolute zero temperature all particles of the system are condensed. Thus, the classic superfluidity of ^{4}He atoms and the superconductivity of Cooper electronic pairs are essentially quantum phenomena existing near the absolute zero temperature.

One can ask: Is it possible to force fluid particles to move collectively without quantum Bose condensation? After all, atoms and molecules of most liquids are not bosons, and most liquids composed of bosons have the freezing temperature higher than the Boson condensation temperature T_0. It is obvious that this cannot be implemented in a bulk phase of any liquid because of a chaotic motion of its atoms (molecules). However, in the case of a strong confinement inside a certain nanochannel with boundary walls having the crystalline structure, this structure can induce a spatially ordered liquid one. Under action of an external driving force this spatially ordered fluid should move as a whole, and this collective movement of fluid particles could exhibit some semblance of the superfluidity. Due to the crystalline honeycomb-like structure of bounding walls, carbon nanotubes (CNTs) seem to be most suitable candidates for the role of such nanochannels.

There are two types of CNTs, namely, single-walled carbon nanotubes (SWCNTs) and multi-walled carbon nanotubes (MWCNTs) which are structures composed of several concentric SWCNTs with different chiral angles [2–6]. Diameters of CNTs range from a few to tens of nanometers, and their lengths may reach several microns [7–10]. In addition, in [11], a possibility of formation of CNTs with rectangular cross sections was discussed, and, recently, it was reported in [12] that such carbon nanotubes can be really formed. Both SWCNTs and MWCNTs exhibit superior mechanical, electronic, thermal, and transport properties [13–27]. For example, experimental investigations and computer simulations revealed that pressure drop driven fluid flows through CNTs could be four to five orders of magnitude faster relative to predictions of classic hydrodynamics [16,22]. Thus, due to their unique properties, during the last 20–30 years, CNTs attract a huge

*Corresponding author: miran@mail.ru; www.ipme.ru

interest of the international research community and they are widely used in many electronic, medical, space, and military applications [28–30].

All above-mentioned computer simulations of fluid structures inside common CNTs with circular cross sections revealed that fluid atoms (molecules) form either one-dimensionally ordered chains or structures in which fluid particles are disposed on coaxial cylindrical surfaces. In our previous paper [31], using molecular dynamics (MD) simulation, we studied behavior of polar and nonpolar liquids confined by SWCNT with square cross section and showed that fluid inside such SWCNT exhibits spatially ordered equilibrium structure which resembles the shape and structure of bounding walls. Therefore, one can expect that under action of an external driving force such spatially ordered fluid structures could move as a whole and exhibit some semblance of the superfluidity. It is obvious that this opportunity should be investigated

In the present paper, using MD simulations, we study equilibrium structures and flows of argon atoms confined by SWCNTs having the circular cross section and the rectangular one with a ratio between its sides 1 : 4. Both these nanotubes have the same length and cross section area. We chose MD simulations of the nonpolar argon atom flows through these SWCNTs for two reasons. First, interactions between argon atoms are well described by the short-range Lennard-Jones (LJ) potential which is very convenient for MD simulations. Second, our previous simulations [31] revealed that inside SWCNTs equilibrium structures formed by nonpolar atoms are significantly more spatially ordered than those formed by polar molecules such as water ones. As said above, we expect that more spatially ordered atomic structures inside SWCNTs should be better candidates for demonstration of the collective movements. It has been found that, under action of external driving forces, the spatially ordered structures formed by argon atoms inside such nanotubes really move as solid objects, i.e., collectively. It has been also revealed that there are two regimes of such collective movement. In the first regime, when the driving external force f_{x0} is lower than a certain critical value f_{xc}, the retarding friction force f_{Rx} acting on fluid particles from the bounding walls becomes equal to f_{x0}, and the average flow velocity reaches some saturated finite value. In the second regime, when the driving external force f_{x0} exceeds f_{xc}, the retarding friction force f_{Rx} gradually drops to zero and the average flow velocity exhibits an unlimited growth. Moreover, when the retarding friction force f_{Rx} becomes infinitely small, one can switch off the external driving force and the fluid will continue to flow at the same constant velocity. Thus, the second regime of the flow through above mentioned SWCNTs resembles the superfluidic liquid flow.

II. SIMULATION DETAILS

Using MD simulations, we investigate flows of argon atoms confined by carbon nanotubes with common circular cross section and rectangular one having the ratio between its sides 1 : 4. The lateral projections and cross sections of these SWCNTs are shown in Figs. 1(a) and 1(b), respectively. All these carbon nanotubes have the same length $L = 7.48$ nm

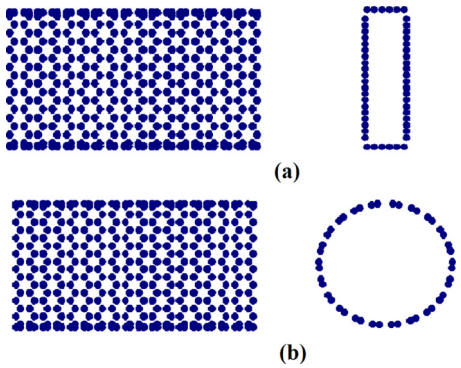

FIG. 1. The lateral projections (the tube axes are parallel to the x axis) and cross sections of SWCNTs used in our MD simulations. (a) SWCNT with rectangular cross section and with the ratio between its sides 1 : 4; (b) SWCNT with circular cross section.

and the cross section area $S = 1.77$ nm^2, and their bounding walls have the graphene crystalline structure. Argon atoms are considered as point-like particles which interact with each other via the short-range LJ pairwise potential

$$U_{LJ}(r_{ij}) = 4\epsilon_{ij}\lceil(\sigma_{ij}/r_{ij})^{12} - (\sigma_{ij}/r_{ij})^{6}\rceil, \qquad (1)$$

where ϵ_{ij} and σ_{ij} are the strength and characteristic length, respectively, for the LJ interaction between ith and jth atoms, and r_{ij} is the distance between them. These constants for argon atoms, ϵ_{Ar} and σ_{Ar}, are well known [32], and they are equal to $\epsilon_{\mathrm{Ar}} = 1.653 \times 10^{-14}$ erg and $\sigma_{\mathrm{Ar}} = 3.405$ Å, respectively. An interaction between argon atoms and carbon atoms of SWCNTs is described by the LJ potential similar to Eq. (1) in which the interaction constants ϵ_{Ar} and σ_{Ar} are replaced by $\epsilon_{\mathrm{CAr}} = 0.661 \times 10^{-14}$ erg and $\sigma_{\mathrm{CAr}} = 3.302$ Å, respectively. All these constants are determined from [23] by means of the Lorentz-Berthelot rules. The total force $\vec{F}_i$ acting on the ith fluid particle due to interactions with other particles, and equations of motion of this particle are given by Eqs. (3),(6) in [33]. All simulations are performed in the NVT ensembles, and, at each time step, the equations of motion of fluid atoms are solved numerically by the standard method described in [34]. The temperature of the systems under consideration is kept constant ($T = 85$ K for liquid phase of argon) by employing the Berendsen thermostat [35] with the time constant ∼0.1 ps that is typical for MD simulations of condensed phase systems. This temperature is calculated from the kinetic energy of the thermal motion of argon atoms. In such calculations, we take into account velocity components $v_y(i)$ and $v_z(i)$ of individual ith argon atom, whereas in x-direction parallel to the SWCNT's axis, we consider a difference $v_x(i) - V_x$, where $v_x(i)$ is the velocity component of individual ith argon atom, and V_x is the average flow velocity. Since the carbon atoms in CNTs are connected to each other with very strong covalent bonds [36] with the interaction constants much larger than the LJ interaction constants ϵ_{CAr}, these atoms are considered to be fixed at their equilibrium sites. This approximation is supported by estimations of thermal vibrations of SWCNTs performed in [37]. According to these estimations, average amplitudes of such vibrations are of the order of ∼0.01 nm which is significantly smaller than typical atomic sizes.

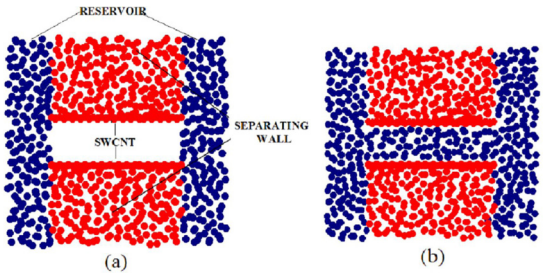

FIG. 2. The lateral projection of initial and final equilibrium configurations considered in our MD simulations. (a) initial configuration; (b) final equilibrium configuration. Blue circles are argon atoms and red ones are carbon atoms.

III. SIMULATION RESULTS AND DISCUSSION

First of all, we obtained equilibrium static structures of argon atoms inside SWCNTs mentioned in the Introduction. In order to obtain these structures, we performed MD simulations of free (without an external pressure drop) permeations of argon atoms into these SWCNTs. These simulations started from the initial configuration schematically depicted in Fig. 2(a). This configuration is made as follows: initially we have two reservoirs of argon atoms separated from each other by the wall consisted of carbon atoms. Then, we make a channel in this wall and insert the corresponding SWCNT into the channel. Now, this SWCNT connects two reservoirs with each other and argon atoms can freely permeate into the SWCNT without any external action. After running during about 10^5 time steps (one time step was equal to 0.001 ps), one can reach the equilibrium configuration schematically shown in Fig. 2(b).

During simulation processes, the system under consideration is placed within the parallelepiped simulation box of $10 \times 10 \times 10$ nm^3 in size, and the periodic boundary conditions [34] were imposed on the system in x, y, and z directions.

Figures 3(a) and 3(b) show lateral projection and cross section, respectively, of equilibrium configuration of argon atoms inside SWCNT with the described above rectangular cross section, and Fig. 3(c) exhibits the corresponding density profile in y direction. From these figures one can conclude that argon atoms inside this SWCNT form the plane parallel to lateral bounding walls and this plane is located in the center of the tube. In addition, the argon atoms within this plane form the structure that resembles the graphene structure of the bounding walls. Figures 4(a) and 4(b) demonstrate the cross section of the structure formed by argon atoms inside SWCNT with circular cross section and the corresponding radial density profile, respectively. From these figures one can conclude that inside this SWCNT some argon atoms form the chain-like structure along the tube axis whereas other argon atoms are disposed on the cylindrical surface coaxial with the bounding walls. The radial distance between such cylindrical surface and bounding wall as well as the distance between this surface and the chain-like structure is equal to about σ_{Ar}. Thus, argon atoms in both SWCNTs form spatially ordered structures.

Now, let us turn to results of MD simulations of argon atom flows through the above mentioned SWCNTs with

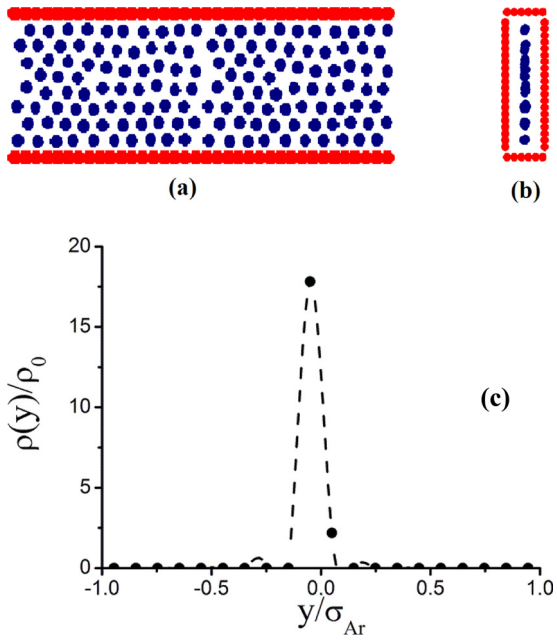

FIG. 3. The lateral projection (a) and cross section (b) of equilibrium structure of argon atoms inside SWCNT with rectangular cross section depicted in Fig. 1(a). Red circles denote the bounding wall carbon atoms and blue circles denote argon atoms. (c) is the corresponding density profile along y axis perpendicular the lateral bounding walls.

circular and rectangular cross sections under action of pressure drops across these nanotubes. To simulate these flows, in the equilibrium configurations depicted in Fig. 2(b), we remove the liquid reservoirs and apply periodic boundary conditions to edges of SWCNTs. The external pressure drop across nanotubes is mimicked by the external force f_{x0} acting on each liquid particle inside SWCNTs. In order to calculate instant average flow velocities V_x along SWCNT axes, we calculate the total fluxes through SWCNTs at each time step and divide these fluxes by numbers of argon atoms inside these nanotubes. At each time step we also calculate the total forces acting on all argon atoms from the bounding walls in x, y, and z directions and divide these forces by numbers of argon atoms inside SWCNTs. It is obvious that the force f_{Rx} obtained in such way for the x direction is an instantaneous

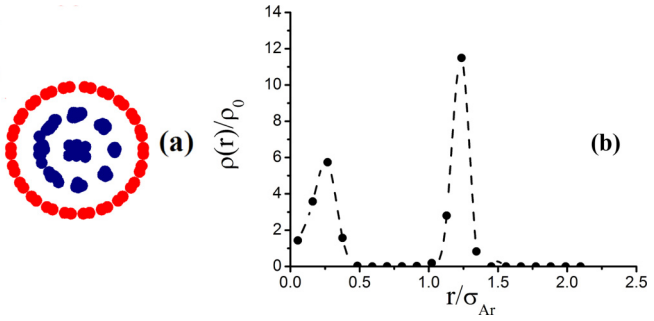

FIG. 4. The cross section of equilibrium structure formed by argon atoms inside SWCNT with circular cross section (a). (b) The corresponding radial density profile.

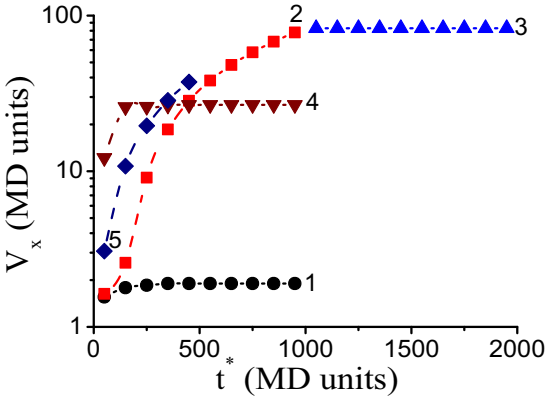

FIG. 5. Time dependencies of average argon flow velocities v_x through SWCNTs with circular and rectangular cross sections. Curve 1: the first regime ($f_{x0} = 0.09$) for SWCNT with circular cross section; curve 2: the second regime ($f_{x0} = 0.1$) for the same SWCNT; curve 3: after switching off the external driving force ($f_{x0} = 0$), circular cross section; curve 4: the argon atom flow through SWCNT with rectangular cross section and bounding wall consisting of carbon atoms randomly distributed on its surface, $f_{x0} = 0.2$; curve 5: $T = 1.24K$, $f_{x0} = 0.09$.

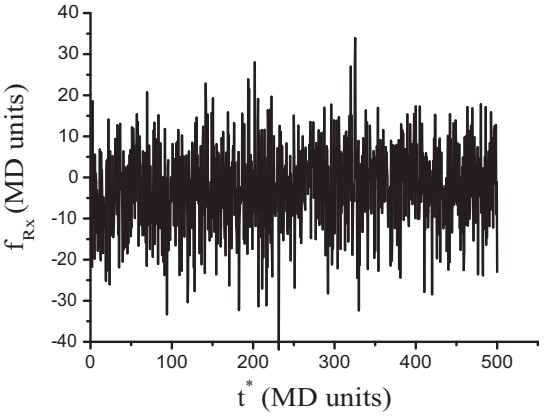

FIG. 6. Typical time dependence of instantaneous retarding force f_{Rx} acting on argon atoms from bounding wall carbon atoms during argon flow through SWCNT with circular cross section

retarding friction force acting on each argon atom from the bounding walls. During the simulation process we follow for the time evolutions of V_x and f_{Rx} and average these values over sufficiently long consecutive time intervals (100 MD time units). Thus, we can study the character of the argon atom transports through the SWCNTs.

The results of our simulations reveal that argon atom flows through SWCNTs under consideration can be really considered as collective movements. Especially clearly the collective character of these flows can be demonstrated by a short movie consisting of successive snapshots of argon atoms moving inside SWCNT with rectangular cross section for $f_{x0} = 0.15$ (see Supplemental Material [38] for movie of collective movement of argon atoms inside SWCNT with rectangular cross section). From this movie one can see that argon atoms move synchronously along x axis parallel to the tube axis. At the same time, they demonstrate thermally induced small oscillations along direction perpendicular to x axis about their equilibrium positions. As we will see later, these oscillations are related to the retarding friction force f_{Rx}.

Our simulations also show that there are two regimes of the argon atom flows through the above mentioned SWCNTs. In the first regime, when the external driving force f_{x0} is smaller than a certain critical value f_{xc}, which for SWCNTs with circular and rectangular cross sections, respectively, is equal to 0.095 and 0.14 (in MD force units $f_{\mathrm{MD}} = \epsilon_{\mathrm{Ar}}/\sigma_{\mathrm{Ar}} = 4.85 \times 10^{-12}N$), argon atoms move through these SWCNTs with steady and finite average flow velocities V_x. It means that, since the external force f_x is switched on, argon atoms begin to move along the tube axis with a certain accelerations until the average fluid flow velocity reaches the steady value V_x. It is clearly seen from Fig. 5, curve 1, which demonstrates the time evolution of V_x averaged over consecutive time intervals with duration equal to 100 MD time units for SWCNT with circular cross section at the driving force $f_{x0} = 0.09$. This is a quite expected behavior of fluid flows through SWCNTs. However, in the second regime, when the driving force f_{x0} exceeds the critical value f_{xc}, the flow velocity V_x averaged over above mentioned consecutive time intervals exhibits an unlimited growth with no signs of saturation (see curve 2 in Fig. 5 for $f_{x0} = 0.1$). Moreover, if we then switch off the external force ($f_{x0} = 0$), the average flow velocity remains constant with no signs of decay (curve 3 in Fig. 5). It should be noted that, for SWCNT with rectangular cross section, we observe qualitatively the same behavior and, therefore, the time dependencies for this nanotube analogous to those depicted in Fig. 5 are not brought here.

In order to understand such extraordinary "superfluidic" behavior of argon atom flows through above mentioned SWCNTs with different cross sections, we must analyze time dependencies of all forces acting on argon atoms during their flows through these SWCNTs. It is obvious that each atom inside SWCNT is subjected to two external forces directed along the tube axis, namely, the external driving force f_{x0} and retarding force f_{Rx} due to interactions between a given atom and bounding wall carbon atoms. The external driving force f_{x0} is constant, and typical time dependence of instantaneous value of f_{Rx} is shown in Fig. 6.

It is easily seen that this time dependence has a stochastic-like character, and we must analyze time averaging of this force over the above mentioned consecutive time intervals. The results of such time averaging for two regimes of argon atom flow trough SWCNT with circular cross section are shown in Fig. 7 which exhibits time dependencies of the ratio $|f_{Rx}|/f_{x0}$, where $|f_{Rx}|$ is the absolute value of the time averaged retarding force f_{Rx}. One can see from this figure that, for the first regime of the argon atom flow ($f_{x0} = 0.09$), the ratio $|f_{Rx}|/f_{x0}$ first grows with time and then reaches saturation at the steady value equal to nearly 1 (curves 1). It means that the absolute value of the time averaged retarding force f_{Rx} becomes equal to the external driving force f_{x0} but it has an opposite sign. As a result, the total force acting on carbon atoms during their flow through SWCNT vanishes, and they move with a certain constant time averaged velocity. One can also see from this figure (curve 2) that, in the second regime of the argon atom flow through SWCNT with circular

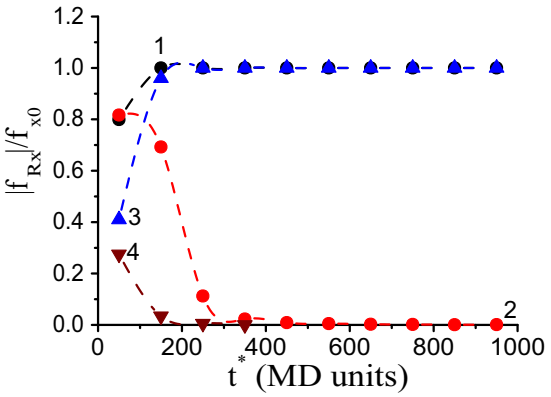

FIG. 7. Time dependencies of the ratio $|f_{Rx}|/f_{x0}$ averaged over consecutive time intervals during the argon atom flows through SWCNTs with circular and rectangular cross sections. Curve 1: the first regime ($f_{x0} = 0.09$), circular cross section; curve 2: the second regime ($f_{x0} = 0.1$), circular cross section; curve 3: the argon atom flow through SWCNT with rectangular cross section and bounding wall consisting of carbon atoms randomly distributed on its surface, $f_{x0} = 0.2$; curve 4: $T = 1.24K$, $f_{x0} = 0.09$.

cross section ($f_{x0} = 0.1$), the ratio $|f_{Rx}|/f_{x0}$ decays with time to nearly zero, and argon atoms begin to move along tube axis in a frictionless ballistic regime which resembles the phenomenon of superfluidity.

There are several questions. The first question is what is the reason for the existence of the above two regimes of flow of argon atoms through SWCNTs? To answer this question we must consider the movement of argon atoms inside SWCNT. As said above, this movement has a collective character when all liquid particles move synchronously along x axis parallel to the tube axis (see movie in Supplemental Material [38]). Therefore, it is sufficient to consider a movement of only one argon atom within the all ensemble in the periodic potential field $U(x, y, z)$ created by the bounding wall carbon atoms. It is obvious that due to the crystalline structure of the graphene bounding walls $U(x + a, y, z) = U(x, y, z)$, where a is the period of this crystalline structure. Then, the averaging over time of the force f_Rx acting on a given argon atom from the bounding wall carbon atoms can be replaced by its spatial averaging along x axis over the period a. It means that

$$f_{Rx} = \frac{1}{a}\int_{x_0}^{x_0+a} f_x dx, \tag{2}$$

where $[x_0, x_0 + a]$ is the interval along x axis which is passed by the our argon atom with the average flow velocity V_x. As seen from the movie in the Supplemental Material [38], an individual argon atom not only moves along x axis with the velocity V_x but also makes a small thermal movement in y and z directions around a certain equilibrium position (y_0, z_0). Then we can write its potential energy as $U(x, y, z) \approx U(x, y_0, z_0) + (\partial U(x, y_0, z_0)/\partial y)\delta y + (\partial U(x, y_0, z_0)/\partial z)\delta z$, where δy and δz are thermal displacements of the argon atom along y and z axes, respectively, relative its equilibrium position (y_0, z_0). Taking into account that $\partial U(x, y_0, z_0)/\partial y$ and $\partial U(x, y_0, z_0)/\partial z$ are the forces $f_y(x, y_0, z_0)$ and $f_z(x, y_0, z_0)$ acting on the argon atom along y and z directions, respectively, from bounding wall carbon atoms, one can write

$$U(x, y, z) \approx U(x, y_0, z_0) + f_y(x, y_0, z_0)\delta y + f_z(x, y_0, z_0)\delta z. \tag{3}$$

Then, taking into account that $f_x = \partial U(x, y, z)/\partial x$, and that, due to the periodicity of the potential energy U, $f_y(x_0 + a, y_0, z_0) = f_y(x_0, y_0, z_0)$ and $f_z(x_0 + a, y_0, z_0) = f_z(x_0, y_0, z_0)$, the integration (2) gives

$$f_{Rx} \approx (1/a)[f_y(x_0, y_0, z_0)(\delta y(x = x_0 + a) - \delta y(x = x_0)) + f_z(x_0, y_0, z_0)(\delta z(x = x_0 + a) - \delta z(x = x_0))]. \tag{4}$$

We can also take $(\delta y(x = x_0 + a) - \delta y(x = x_0)) \approx (v_y/V_x)a$ and $(\delta z(x = x_0 + a) - \delta z(x = x_0)) \approx (v_z/V_x)a$, where v_y and v_z are the rates of thermal motion of the argon atom along y and z directions, respectively. Then, we can finally obtain that

$$f_{Rx} \approx f_y(x_0, y_0, z_0)(v_y/V_x) + f_z(x_0, y_0, z_0)(v_z/V_x). \tag{5}$$

One concludes from this equation that the higher the average flow velocity V_x the smaller the retarding force f_{Rx} acting on the argon atoms from the SWCNT bounding walls and, for $V_x \to \infty$, the retarding force $f_{Rx} \to 0$. This result can explain existence of the second frictionless regime of the argon atom flow through SWCNTs that resembles the phenomenon of superfluidity. As for the first regime of the argon atom flow with retarding friction force different from zero, one can assume that this regime occurs when the external driving force f_{x0} is not sufficiently large to accelerate argon atom flow to a high enough velocity V_x sufficient to reverse the retarding force f_{Rx} to zero. The problem of existence of the critical external driving force f_{xc} now remains unsolved and requires further investigation.

The second question is what is the role of the crystalline structure of the SWCNT bounding walls in occurrence of the frictionless fluid flow through these SWCNTs. The above derivation of Eq. (5) is based on an assumption of periodicity of the potential field $U(x, y, z)$ created by the bounding wall carbon atoms and, hence, one can conclude that the crystalline structure of the SWCNT bounding wall should play an essential role in existence of this phenomenon. In order to check this conclusion, we performed MD simulation of the argon atom flow through SWCNT with the same length and rectangular cross section but with bounding walls consisting of carbon atoms randomly distributed on their surfaces. These simulations show that, for the external driving forces f_{x0} ranging from 0.1 to 0.7 MD force units, the argon atom flows demonstrate only the first regime of flow with the retarding friction force f_{Rx} different from zero. This fact is illustrated by curves 4 and 3 in Figs. 5 and 7, respectively, which show time evolutions of the average flow velocity V_x and the ratio $|f_{Rx}|/f_{x0}$ obtained for $f_{x0} = 0.2$. The third question concerns the role of the temperature for occurrence of the frictionless superfluidic flow through SWCNT. According to Eq. (5), the lower the velocities of thermal motion of argon atoms the smaller should be the retarding friction force f_{Rx}. It means that decreasing the temperature of the system we could obtain the second frictionless regime of the argon atom flows through

SWCNTs at lower values of the critical external driving force f_{xc}. In order to check this conclusion, we performed MD simulations of the argon atom flow through SWCNT with circular cross section at the temperature of the system $T = 1.24$ K and obtained a relatively moderate decrease of the critical external driving force, namely, $f_{xc} = 0.06$. Curves 5 and 4 in Figs. 5 and 7, respectively, show time evolutions of the average flow velocity V_x and the ratio $|f_{Rx}|/f_{x0}$ obtained for $f_{x0} = 0.09$ and $T = 1.24$ K. Combining these results, one can conclude that for $T = 1.24$ K the friction force drops to zero at velocity V_x noticeably lower than that for $T = 85$ K. This fact can be qualitatively explained by that the velocities v_y and v_z are proportional to $T^{1/2}$, and, thus, decreasing temperature from 85 K to 1.24 K, we decrease these velocities by about 8 times.

Finally, let us estimate the external pressure drops required for experimental observation of the predicted here frictionless superfluidic second regime of the argon atom flow through experimentally available SWCNTs. For SWCNT with circular cross section, we obtained $f_{xc} \sim 0.1$ in reduced MD force units f_{MD}. For argon atoms, this value corresponds to $f_{xc} \sim 4.85 \times 10^{-13} N$ per each argon atom inside SWCNT. The SWCNT with circular cross section under our consideration contains 184 argon atoms that gives the total external driving force acting on them equal to $\sim 8.9 \times 10^{-11} N$. Taking into account that our SWCNT has the cross section area equal to 1.77 nm^2 and the length 7.48 nm, one can obtain the corresponding pressure drop $\Delta P/\Delta X \sim 6.7 \times 10^{15}$ Pa/m. Now, let us estimate the minimum SWCNT's length required for observation of the predicted here regime of the frictionless ballistic argon atom flow through this SWCNT. As said above, we simulate the argon atom flow through SWCNT at the periodic boundary conditions, i.e., we assume that our SWCNT has an infinitely large length. In real experiments, however, experimentalists usually use CNTs with finite lengths which are in a contact with a fluid reservoirs and the fluid flows through these CNTs under the action of pressure generated by a certain piston (see for example [20]). Since, as said above, in the second flow regime, the retarding friction force f_{Rx} drops to zero after achievement of some sufficiently large velocity V_x, this process takes some time Δt during which argon atoms pass some distance ΔL. It is clear, that this distance is a minimum SWCNT length required for observation of the predicted here regime of the frictionless ballistic flow. One can find from Fig. 7 that $\Delta t \approx 300$ MD time units. This time unit for argon atoms is equal to $\sigma_{\mathrm{Ar}}/V_{\mathrm{MD}}$, where V_{MD} is the velocity MD unit for argon atoms. From Fig. 5 one can find that, for $\Delta t \approx 300$ MD time units, argon atoms achieve the velocity $\approx 13.3 V_{\mathrm{MD}}$, and, since in the second flow regime the argon atom velocity V_x grows with time practically linearly, the average velocity V_x^{aver} over time interval Δt is equal to $\approx 6,65 V_{\mathrm{MD}}$. Thus, one can easily obtain that $\Delta L \approx 300(\sigma_{\mathrm{Ar}}/V_{\mathrm{MD}}) \times 6,65 V_{\mathrm{MD}} \approx 1995\sigma_{\mathrm{Ar}}$, or $\Delta L \approx 680$ nm. Then, the pressure drop required for observation of regime of the frictionless ballistic argon atom flow through SWCNT with such length can be estimated as $\sim 6.7 \times 10^{15} \times 680 \times 10^{-9} \sim 4600$ MPa. The estimated here required SWCNT length is typical for CNTs used in experiments. However, the required pressure drop is very large. For example, the pressure drop used in experiments on filling of CNTs with water was ~ 80 MPa [39]. The author of this paper is not experimentalist and, therefore, he has no information about the capabilities of the necessary experimental equipment nowadays. However, it should be noted that the ballistic frictionless gas flow through two-dimensional channels made from graphene or boron nitride has been recently observed [40].

IV. CONCLUSION

We performed MD simulations of equilibrium structures and flows of argon atoms confined by SWCNTs with circular cross section and rectangular cross sections having the same area and the ratio between its sides 1 : 4. It has been shown that, inside these SWCNTs, argon atoms form the spatially ordered structures and,under action of external driving forces directed along SWCNT axes, they move collectively. Argon atoms move synchronously along x axis parallel to the SWCNT axis and, at the same time, they demonstrate thermally induced small oscillations along directions perpendicular to x axis about their equilibrium positions. It has been also revealed that there are two regimes of such collective movement. In the first regime, when the driving external force f_{x0} is lower than a certain critical value f_{xc}, the retarding friction force f_{Rx} acting on fluid particles from the bounding walls becomes equal to f_{x0}, and the average flow velocity reaches some saturated finite value. In the second regime, when the driving external force f_{x0} exceeds f_{xc}, the retarding friction force f_{Rx} gradually drops to zero and the average flow velocity exhibits an unlimited growth. Moreover, when the retarding friction force f_{Rx} becomes infinitely small, one can switch off the external driving force and the fluid will continue to flow at the same constant velocity. Thus, in the second regime, argon atoms inside the above mentioned SWCNTs demonstrate the ballistic frictionless flows which resemble the superfluidic liquid flow. A simple semi quantitative explanation of this phenomenon is brought. It has been shown that collective frictionless ballistic flows of argon atoms through SWCNTs are caused by the crystalline structure of SWCNT's bounding walls and, for the same SWCNTs with random distribution of carbon atoms on the bounding walls, one can observe only the first regime of argon atom flows. The minimum SWCNT length and the pressure drop required for an observation of the frictionless ballistic argon atom flows are estimated. Finally, it should be noted that the ballistic frictionless flows through SWCNTs could be, in principle, demonstrated not only by argon atoms but also by other atoms and molecules. It is clear that these possibilities require further investigations.

ACKNOWLEDGMENT

The author is very grateful to Prof. A. K. Abramyan for useful discussions.

[1] D. R. Tilley and J. Tilley, *Superfluidity and Superconductivity*, 3rd ed. (CRC Press, Boca Raton, FL, 1990).

[2] S. Iijima, Nature **354**, 56 (1991).

[3] B. I. Yakobson and R. E. Smalley, Am. Sci. **85**, 324 (1997).

[4] E. T. Thostenson, Z. F. Ren, and T. W. Chou, Compos. Sci. Technol. **61**, 1899 (2001).

[5] D. Qian, G. F. Wagner, W. K. Liu, M. F. Yu, and R. S. Ruoff, Appl. Mech. Rev. **55**, 495 (2002).

[6] C. Y. Wang, Y. Y. Zhang, C. M. Wang, and V. B. C. Tan, J. Nanosci. Nanotech. **7**, 4221 (2007).

[7] D. S. Bethune and C. H. Kiang, Nature **363**, 605 (1993).

[8] M. S. Dresselhaus, G. Dresselhaus, and R. Saito, Carbon **33**, 883 (1995).

[9] T. W. Ebbesen, Phys. Today. **49**(6), 26 (1996).

[10] M. S. Dresselhaus, G. Dresselhaus, and P. Avouris, *Carbon Nanotubes* (Clarendon Press, Oxford, 1989).

[11] P. A. S. Autreto, S. B. Legoas, M. Z. S. Flores, and D. S. Galvao, J. Chem. Phys. **133**, 124513 (2010).

[12] K. Mizutani and H. Kohno, Appl. Phys. Lett. **108**, 263112 (2016).

[13] P. G. Collins and P. Avouris, Sci. Amer. **283**, 62 (2000).

[14] G. Hummer, J. C. Rasaiah, and J. P. Nowryta, Nature **414**, 188 (2001).

[15] J. K. Holt, H. P. Park, Y. Waang, M. Staderman, A. B. Artyukhin, C. P. Grigopopulos, A. Noy, and O. Bakajin, Science **312**, 1034 (2006).

[16] M. Majumder, N. Chopra, R. Andrews, and B. J. Hinds, Nature **438**, 44 (2005).

[17] M. Majumder, N. Choudhury, and S. K. Ghosh, J. Chem. Phys. **127**, 054706 (2007).

[18] N. Choudhury and B. M. Pettitt, J. Phys. Chem. **109**, 6422 (2005).

[19] B. Mukherjee, P. K. Maiti, C. Dasgupta, and A. K. Sood, J. Chem. Phys. **126**, 124704 (2007).

[20] M. Whitby, L. Cagnon, M. Thanou, and N. Quirke, Nano Lett. Chem. Lett. **8**, 2632 (2008).

[21] M. Melillo, F. Zhu, M. A. Snyder, and J. Mittal, J. Phys. Chem. Lett. **2**, 2978 (2011).

[22] W. D. Nicholls, M. K. Borg, D. A. Lockerby, and J. M. Reese, Microfluid. Nanofluid. **12**, 2578 (2012)

[23] N. Chopra and N. Choudhury, J. Phys. Chem. C. **117**, 18398 (2013).

[24] S. K. Kannam, B. D. Todd, J. S. Hansen, and P. Davis, J. Chem. Phys. **138**, 094701 (2013).

[25] J. Su and K. Yang, Chemphyschem. **16**, 3488 (2015).

[26] X. Meng and J. Huang, Mol. Simul. **42**, 215 (2015).

[27] A. Sam, S. K. Kannam, R. Hartkamp, and S. P. Sathian, J. Chem. Phys. **146**, 234701 (2017).

[28] M. E. Suk and N. R. Aluru, Nano. Micro. Thermophys. Eng. **21**, 247 (2017).

[29] S. J. Klaine, P. J. J. Alvarez, G. E. Batley, T. F. Fernandes, R. D. Handy, D. Y. Lyon, S. Mahendra, M. J. McLaughlin, and J. R. Lead, Environ. Phys. Toxicol. Chem. **29**, 1825 (2008).

[30] M. S. Mauter and M. Elimelech, Sci. Technol. **42**, 5843 (2008).

[31] A. K. Abramyan, N. M. Bessonov, L. V. Mirantsev, and A. A. Chevrychkina, Eur. Phys. J. B. **91**, 48 (2018).

[32] J. A. White, J. Chem. Phys. **111**, 9352 (1999).

[33] L. V. Mirantsev and M. L. Lyra, Phys. Lett. A **380**, 1318 (2016).

[34] M. P. Allen and D. J. Tildesly, *Computer Simulations of Liquids* (Clarendon Press, Oxford, 1989).

[35] H. J. C. Berendsen, J. P. M. Postma, W. F. van Gunsteren, A. DiNola, and J. R. Haak, J. Chem. Phys. **81**, 3684 (1984).

[36] J. Tersoff, Phys. Rev. B **37**, 6991 (1988).

[37] L. Wang and H. Hu, Proc. Math. Phys. Eng. Sci. **470**, 20140087 (2014).

[38] See Supplemental Material at http://link.aps.org/supplemental/10.1103/PhysRevE.100.023106 for a movie of collective movement of argon atoms inside SWCNT with rectangular cross section.

[39] N. Naguib, H. Ye, Y. Gogots, A. G. Yazicioglu, C. M. Megaridis, and M. Yoshimura, Nano Lett. **4**, 2237 (2004).

[40] A. Keerthi, A. K. Geim, A. Janardanan, A. P. Rooney, A. Esfandiar, S. Hu, S. A. Dar, I. V. Grigorieva, S. J. Haigh, F. C. Wang, and R. Radha, Nature **558**, 420 (2018).